Synthetic Insertion of Gold Nanoparticles into Mesoporous Silica

Zoltán Kónya,[†,‡] Victor F. Puntes,[†,‡] Imre Kiricsi,[†,‡] Ji Zhu,[†,‡] Joel W. Ager, III,[‡] Moon Kyu Ko,[§] Heinz Frei,[§] Paul Alivisatos,[†,‡] and Gabor A. Somorjai*[,†,‡]

Department of Chemistry, University of California at Berkeley, Berkeley, California 94720, and Materials Sciences Division, MS 62-203, and Physical Biosciences Division, MS 3-0232, 1 Cyclotron Road, Lawrence Berkeley National Laboratory, Berkeley, California 94720

Received August 9, 2002. Revised Manuscript Received December 18, 2002

Industrial catalysts often consist of transition metals supported on microporous or mesoporous high surface area oxides and are prepared by techniques such as impregnation and ion adsorption. In standard fabrication processes the metal particle size is not well-controlled. In this paper we report a new synthetic route for the production of catalyst materials with more precise control of the metal particle size. Gold nanoparticles encapsulated in mesoporous silica (MCM-41 and MCM-48) served as a model system, although the techniques described are applicable to a wide variety of metals and oxide supports. The samples were characterized by a combination of low-angle powder X-ray diffraction, transmission electron microscopy, N_2 porosimetry, infrared spectroscopy, and X-ray absorption near-edge spectroscopy. The results show that the MCM-41 and MCM-48 structures retain their long-range order when metal particles are added; in addition, the size of the channels increases monotonically with metal loading. X-ray absorption near-edge spectroscopy in combination with the adsorption of thiols provides conclusive evidence that 2- and 5-nm-diameter Au nanoparticles are incorporated into the pores of the silicates and that they are accessible to reactant molecules.

Introduction

An important goal of catalysis science is to understand the factors influencing reaction selectivity and then use this knowledge to prepare catalysts that are selective toward formation of a desired product. Surface science and catalytic reaction studies have identified the structure of the surface of the catalyst as one of the main parameters that controls selectivity.[1] Alterations in selectivity are often produced by changes of catalyst particle size or changes in defect concentrations, such as the presence of steps and kinks. These structural features can be tuned when metallic single crystals are used as model catalysts, which in some cases, allow careful control of the desired catalytic process.

Thus, the preparation of metal nanoparticles within inorganic matrixes possessing pore structures of molecular dimensions has been the subject of catalyst research and development for decades. The production of these types of catalysts leads to high surface area systems in which (i) the shape-selective behavior of porous materials can be combined with the catalytic action of metal particles; this cannot be done for amorphous oxide-supported metal catalysts. (ii) If the particles can be made with a uniform size distribution, this may improve reaction selectivity. (iii) The catalytic activity and selectivity of nanometer-sized metal particles might be very different from that of larger metal islands.

Literature data are available on the preparation of bifunctional metal-loaded zeolite catalysts. The general procedures used are as follows:

(i) Ion exchange of the transition or noble metal ions into the zeolite followed by reduction. For this method, metal atoms are initially generated adjacent to the ion exchange position of the framework and these atoms subsequently form clusters while moving toward the outer surface. As long as the size of the cluster is smaller than the pore, it may be encapsulated in the pore system. However, the distribution of particles is generally not uniform and the metal component can be found both inside the pores and on the outer surface. The advantage of this method is that the amount of metal ions can be regulated up to the ion exchange capacity of the silicate.[2]

(ii) Chemical vapor deposition (CVD) has also been used to deposit metal particles in and on zeolites or mesoporous materials. Metal particles are formed by CVD due to the attachment of the metal precursor (generally a metal complex such as a carbonyl) to the outer surface of the support material, where it subsequently decomposes. The amount of metal that can be introduced by this procedure is limited by the pore volume of the support material. This method may be

* Corresponding author. E-mail: somorjai@socrates.berkeley.edu. Fax: (510) 643-9668.
† University of California at Berkeley.
‡ Materials Sciences Division, Lawrence Berkeley National Laboratory.
§ Physical Biosciences Division, Lawrence Berkeley National Laboratory.

(1) Somorjai, G. A.; Borodko, Y. G. *Catal. Lett.* **2001**, *76*, 1.

(2) Yang, C. M.; Sheu H. S.; Chao, K. J. *Adv. Funct. Mater.* **2002**, *12*, 143.

10.1021/cm020824a CCC: $25.00
Published on Web 02/21/2003

advantageous in some cases, for instance, in the case of non-ion-exchanger porous materials. For these catalysts, the metal particles are attached to both the interior and exterior of the matrix.[3]

(iii) Wet preparation techniques such as incipient wetness and impregnation are generally used for the preparation of supported metal catalysts. However, these methods only rarely (and often accidentally) give uniform distributions of metal particles. This lack of control ensures that the production of metal particles exclusively within the pores of a support material is unlikely.[4]

To prepare a supported catalyst, for which each metal particle has the same size, shape, and crystal structure and they reside exclusively inside the pore system of the matrix, one can first prepare metal nanoparticles in solution with uniform and narrow size distribution and then synthesize the ordered silicate pore system around the metal nanoparticles, thus maximizing the possibility of meeting the above-described requirements. Supported Au nanoparticles represent a particularly interesting system to study, partly due to the recent recognition of excellent low-temperature CO oxidation,[5] hydrocarbon hydrogenation,[6] low-temperature hydrocarbon oxidation,[7] NO reduction activity,[8] and so forth, partly due to the availability of monodispersed Au nanoparticles with sizes ranging from 2 to 100 nm.[9]

The most relevant literature data concerning Au encapsulated in SiO_2 can be summarized as follows. Caruso described some methods for the engineering of nanoparticle surfaces.[10] It was demonstrated that gold nanoparticles could be coated with a silica shell via the reaction of citrate-stabilized gold nanoparticles and alkylaminotrimethoxysilane, followed by polymerization after the addition of a sodium silicate solution. Liz-Marzan, Griersig, and Mulvaney[11] claimed that the preparation of a silica coating on gold nanoparticles was successful only when the gold complexing and silane-coupling agent ((3-aminopropyl)trimethoxysilane) was previously attached to the particle surface. Mann and co-workers[12] prepared functionalized silica shells over gold nanoparticles and showed that the colloidal solutions of these particles were stable for up to 2 months. Methods for covering the surface of gold nanoparticles with polymers have also been discussed.[13] Liz-Marzan and co-workers reported the homogeneous incorporation of silica-coated gold particles into a transparent silica gel without any aggregation of particles.[14] These core−shell nanoparticles are stable and ready for further applications; however, they generally have a nonordered porous shell. Recently, we proposed a simple but very promising method to synthesize controlled size and shape Pt nanoparticles containing mesoporous materials.[15]

To our knowledge, there are no reports describing the preparation of mesoporous silica materials in the presence of different sizes and concentrations of gold nanoparticles with the goal of incorporating the gold particles into the channel system of the mesoporous materials and to investigate the effect of the encapsulation on the silica structure. In this paper we report the results obtained by synthetic insertion of gold nanoparticles in mesoporous silica materials MCM-41 and MCM-48. Two- and five-nanometer gold particles were encapsulated in the two types of zeolites. When 20-nm gold particles were used, they were too large to be able to insert into the pores.

Experimental Section

Materials. Colloidal solutions of gold nanoparticles with diameters of 2, 5, and 20 nm, obtained from Ted Pella Inc. (Redding, CA), were used. These solutions were generally used as received; however, concentration by simultaneous filtering and centrifugation was performed in some cases. The concentrations of the gold nanoparticles in the original solutions were 1.5×10^{14}, 5×10^{13}, and 7×10^{11} particles/mL for particle sizes of 2, 5, and 20 nm, respectively.

We have used gold nanoparticles of these sizes specifically since (i) the 2-nm particles can be easily incorporated into the interior channels of the MCM silicates, (ii) the 5-nm particles are of sufficient size to be considered a borderline case in that they may or may not enter the channels, and (iii) the 20-nm particles should be prevented from entering the pores due to their large size and are thus assumed to be deposited only on the outer surface of the mesoporous silicate.

Synthesis Procedure of Gold-Containing Mesoporous Silica Materials. MCM-41 and MCM-48 mesoporous silicates with regular, one-dimensional, and two-dimensional channel systems in hexagonal and cubic arrangements, respectively, were the target silicates in this study since the pore sizes can be varied from 2.5 to 10 nm. However, these mesoporous materials become less stable as the pore diameter increases due to pore collapse.

The synthesis of mesoporous silicates containing gold nanoparticles was performed utilizing modified versions of procedures described previously. For production of MCM-48 samples, the basic method described by Morey[16] was used. Cetylbenzyldimethylammonium chloride (19 mmol) was dissolved in 9.5 mol (where mol refers to the amount of water) of the appropriate aqueous solution of gold particles. The pH was raised to 13 by the addition of 20 mL of 2 M aqueous tetramethylammonium hydroxide. Then, 50 mmol of TEOS was added and the reaction mixture was rapidly stirred for 2 h. The mixture was then transferred to a 500-mL Teflon bottle and placed in an oven at 85−90 °C for 15 days. The resulting material was washed with distilled water, dried, and subse-

(3) Raja, R.; Sankar, G.; Hermann, S.; Shephard, D. S.; Bromley, S.; Thomas, J. M.; Johnson, B. F. G. *Chem. Commun.* **1999**, 1571.
(4) Han, Y.-J.; Kim, J. M.; Stucky, G. D. *Chem. Mater.* **2000**, *12*, 2068. Lee, K.-B.; Lee, S.-M.; Cheon, J. *Adv. Mater.* **2001**, *13*, 517.
(5) Lin, S. D.; Bollinger, M.; Vannice, M. A. *Catal. Lett.* **1993**, *17*, 245. Lee, S. J.; Gavriilidis, A. *J. Catal.* **2002**, *206*, 305.
(6) Okumura, M.; Akita, T.; Haruta, M. *Catal. Today* **2002**, *74*, 265. Sarkany, A.; Horvath, A.; Bech, A. *Appl. Catal. A* **2002**, *229*, 117. Milone, C.; Tropeano, M. L.; Gulino, G.; Neri, G.; Ingoglia, R.; Galvagno, S. *Chem. Commun.* **2002**, *N8*, 868.
(7) Blick, K.; Mitrelias, T. D.; Hargreaves, J. S. J.; Hutechings, G. J.; Joyner, R. W.; Kiely, C. J.; Wagner, F. E. *Catal. Lett.* **1998**, *50*, 211. Grisel, R. J. H.; Kooyman, P. J.; Nieuwenhuys, B. E. *J. Catal.* **2000**, *191*, 430.
(8) Salama, T. M.; Ohnishi, R.; Shido, T.; Ichikawa, M. *J. Catal.* **1996**, *162*, 169.
(9) Beesley, J. E. *Colloidal Gold. A new perspective for cytochemical marking*; Royal Microscopical Society Handbook No. 17, Oxford Science Publication; Oxford University Press: Oxford, 1989.
(10) Caruso, F. *Adv. Mater.* **2001**, *13*, 11.
(11) Liz-Marzan, L. M.; Griersig, M.; Mulvaney, P. *Langmuir* **1996**, *12*, 4339.
(12) Hall, S. R.; Davis, S. A.; Mann, S. *Langmuir* **2000**, *16*, 1454.
(13) Marinakos, S. M.; Novak, J. P.; Brousseau, L. C.; House, A. B.; Edeki, E. M.; Feldhaus, J. C.; Feldheim, D. L. *J. Am. Chem. Soc.* **1999**, *121*, 8515.
(14) Kobayashi, Y.; Correra-Durante, A.; Liz-Marzan, L. M. *Langmuir* **2001**, *17*, 6375.
(15) (a) Kónya, Z.; Puntes, V. F.; Kiricsi, I.; Zhu, J.; Alivisatos, A. P.; Somorjai, G. A. *Catal. Lett.* **2002**, *81*, 137. (b) Kónya, Z.; Puntes, V. F.; Kiricsi, I.; Zhu, J.; Alivisatos, A. P.; Somorjai, G. A. *Nano Lett.* **2002**, *2*, 907.
(16) Morey, M. S. *Chem. Mater.* **2000**, *12*, 3435.

Table 1. List of Samples and Their Physical Characteristics

sample	Au particle size (nm)	Au particle number (particles/g)	BET[a] (m^2/g)	pore diameter (nm) porosimetry[b]	pore diameter (nm) PXRD[c]	wall thickness[d] (nm)
S-1 (MCM-48)	no gold		895	2.73	2.83	0.61
S-2 (MCM-48)	2	8.5×10^{15}	978	2.73	2.88	1.02
S-3 (MCM-48)	5	2.8×10^{14}	887	2.74	2.84	0.87
S-4 (MCM-48)	20	3.9×10^{12}	981	2.74	2.84	0.92
T-1 (MCM-41)	no gold		751	4.29	3.65	1.04
T-2 (MCM-41)	2	8.6×10^{15}	727	4.29	3.68	0.87
T-3 (MCM-41)	5	2.8×10^{15}	786	3.81	3.54	0.71
T-4 (MCM-41)	20	4.0×10^{13}	829	4.29	3.65	0.96

[a] Specific surface area. [b] Channels diameter calculated from N_2 porosimetry. [c] Channels diameter calculated from PXRD. [d] Thickness of the silica walls.

quently calcined at 550 °C for 6 h to remove the template. To obtain samples with increased gold content, a 50-fold concentrated gold nanoparticle solution was prepared from the 5-nm particle size solution. The MCM-48 samples are designated as S-samples in Table 1.

For the preparation of MCM-41 samples, the procedure of Tuel[17] was used. Solution A contained 0.3 mol of hexadecylamine and 36 mol of aqueous solution of the appropriate gold nanoparticles. Solution B contained 6 mol of ethanol, 1 mol of 2-propanol, and 1 mol of TEOS. The solutions were combined while stirring at room temperature. After being stirred for 1 h, the material was aged and crystallized for 12 h followed by filtration or centrifugation to separate the solid product. The solid product was washed with distilled water and dried. Template removal was performed by heating to 550 °C with a 1 °C/min heating rate followed by treatment at 550 °C for 6 h. As described for the MCM-48 case, a sample has been prepared using a concentrated gold solution. The MCM-41 samples are denoted as T-samples in Table 1.

Samples of both parent materials, MCM-48 and MCM-41, without Au nanoparticles were prepared as described originally for comparative purposes. Additional reference materials were also prepared by simple mechanical mixing of gold particles and the respective mesoporous silicates. A calculated amount of gold solution was mixed with 0.5 g of MCM-41 and MCM-48 silicates. After being stirred for 30 min, the mechanical mixture was dried at 90 °C and powdered.

Measurements. The samples were examined by TEM at the National Center for Electron Microscopy at Lawrence Berkeley National Laboratory, on a JEOL 200CX electron microscope operating at 200 kV. The samples were ground to a fine powder and diluted in methanol to give a 1:3 volume ratio. A Cu grid covered with a 3−4-nm-thick film of amorphous carbon was dipped in the methanol slurry and then allowed to dry covered by a watch glass.

Powder X-ray diffraction (PXRD) was performed on a Bruker-AXS D8 general area detector diffraction system (GADDS), using Co Kα radiation (1.79 Å). The instrument resolution is 0.05° in 2θ and the accumulation time for each sample was at least 20 min at wide angles and 2 min at small angles. PXRD samples were prepared by depositing the powder either on a quartz plate for wide-angle measurements or introducing the fine powder in a 0.5-mm quartz capillary for small-angle measurements. Additional high-resolution data were obtained on the small-angle X-ray scattering (SAXS) beamline 1-4 at the Stanford Synchrotron Radiation Laboratory (SSRL). The incident wavelength was 1.488 Å, and the powder samples were studied in transmission in the q range of 0.2−2.3 nm^{-1}. Typical collection times were less than 5 min.

Nitrogen porosimetry data were collected using a Quantachrome Autosorb 1 surface area analyzer with 60-point analyses at a temperature of 77 K. Template-free samples were pretreated at 393 K for 8 h in a vacuum immediately prior to data collection. Surface areas were calculated using the BET adsorption−desorption method[18] and pore size distributions were analyzed by the BJH method.[19]

FT-infrared spectra of methyl acetylene adsorbed onto pressed wafers of AuMCM-41 or AuMCM-48 were recorded in transmission mode with a Bruker spectrometer model Vector 33. The wafers were mounted inside a miniature infrared vacuum cell equipped with CaF_2 windows. Prior to loading of methylacetylene through a vacuum manifold, the sieve was dehydrated by evacuation with a turbo molecular pump.

The X-ray absorption near-edge structure (XANES) of the sulfur K-edge of cyclohexyl mercaptan and *tert*-butyl mercaptan adsorbed onto AuMCM-48 materials was recorded at beamline 9.3.1 at the ALS. The beamline is equipped with a Si(111) double-crystal monochromator, and the ring runs at 1.9 GeV with a beam current of 200−400 mA. Measurements were conducted in the fluorescence mode using a Si photodiode Hamamatsu model 3584-02 at a 45° angle relative to the incident X-ray beam. The beam intensity was monitored by the current generated at an Al foil. AuMCM-48 samples were used in the form of pressed wafers (10 mg) and mounted on an OFC holder that can simultaneously accommodate 12 samples. The rotatable holder was inserted into the high-vacuum XAFS end station. After evacuation to $<10^{-7}$ Torr, XANES spectra of the thiol-exposed AuMCM-48 wafers were recorded at room temperature in the range 2400−2600 eV at sampling intervals of 1 eV and a recording time of 2 s per data point.

Results and Discussion

The characterization of nanoparticles requires highly sophisticated analytical tools. Such tools are especially appropriate for those cases where the metal nanoparticles are inserted within a solid matrix. The case becomes even more complex when the metal particles are expected to be in the pore system of the solid and accessible for adsorbate or reactant molecules. In the latter case, generally a combination of analytical techniques results in the best characterization. Here, a wide variety of characterization techniques was used to establish whether (i) the gold particles did incorporate into the solid phase. (ii) Was there any influence of gold addition into a reacting gel on the structural ordering of the silicate? (iii) Are the gold nanoparticles located in the pores or on the outer surface of the materials? However, with use of several different characterization techniques (nuclear magnetic resonance spectroscopy, UV−vis spectroscopy, UV−Raman spectroscopy, etc.), the results have not shown any evidence for the successful encapsulation of the gold particles; thus, these techniques are not suitable for answering the questions

(17) Tuel, A. *Chem. Mater.* **1996**, *8*, 114.

(18) Brunauer, S.; Emmett, P. H.; Teller, E. *J. Am. Chem. Soc.* **1938**, *60*, 309.

(19) Barrett, E. P.; Joyner, L. G.; Halenda, P. P. *J. Am. Chem. Soc.* **1951**, *73*, 373.

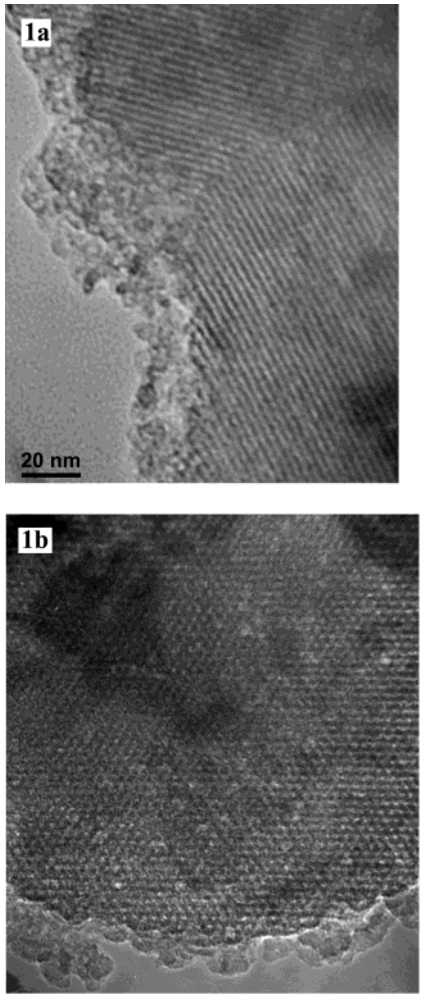

Figure 1. Transmission electron micrographs of the T-1 MCM-41 mesoporous structure: side view (a) and top view (b).

mentioned above. Finally, combined TEM, PXRD, nitrogen porosimetry, FT-IR, and XANES data seemed to be useful for characterizing the gold-containing mesoporous silica structures.

TEM Results. Typical TEM images of the mesoporous structures are depicted in Figure 1. The images show an ordered silicate structure. Figure 1a shows a uniform hexagonal arrangement of bright dots corresponding to the straight channels of MCM-41. Since TEM pictures are projected along the incident beam direction, the real pore diameter may be somewhat less than the actual value. From Figure 1b more reliable pore diameter values can be calculated (Table 1), on the assumption that the channels are cylindrical.

PXRD Results. The products synthesized with 5- and 20-nm gold particles were rose in color whereas samples containing 2-nm gold particles or no gold were colorless, even upon template removal. Samples possessing a higher amount of gold were purple in color. The reference materials of low gold concentrations that were prepared by the mechanical mixture method were light yellow in color whereas the material containing a large amount of 20-nm gold particles was deep violet in color.

The pore diameters of the gold-containing mesoporous silicates, as determined from the PXRD measurements, are listed in Table 1. The change in the reflection intensity upon template removal was small; the peaks were shifted to lower angles, showing a 2−3% collapse

Table 2. Characterization of 2-nm Au Containing MCM-41 Samples

Au concentration (particles/g)	a_0 (nm)	d (nm)	interparticle distance (nm)
no gold	3.93	3.41	
4.5×10^{13}	4.02	3.48	481
4.5×10^{14}	4.05	3.51	223
4.5×10^{15}	4.13	3.58	104

of the channels. Thus, it follows that heat treatment at 823 K did not result in significant structural damage. Besides, it is seen that addition of gold nanoparticles to the reacting gel influences only slightly the ordered structure of the silicates. In cases where much higher amounts of gold particles were used, the ordered character of the samples decreased.

To investigate the flexibility of the silica structure, a series of MCM-41 samples were prepared by varying the Au concentration from 4.5×10^{13} to 4.5×10^{15} particles per 1 g of silica (representing roughly from 1:2000 to 1:20 particle:channel ratio) while keeping the particle size constant (2 nm). As the Au concentration is increased, the XRD peaks are shifted toward smaller angles and the peak broadness remains similar (Table 2). This suggests that the structure expands when particles are included, and the template channels increase regularly to accommodate the structure, due to strong tendency of forming regular channels,[20] instead of becoming a bumpy structure with similar lattice spacing but with lower crystal quality (Figure 2). In addition, it seems that the presence of these expanded channels determines the lattice spacing of the self-assembly; that is, the hexagonal structure would be strained if the channels had a distribution of diameters. Thus, a progressive shift toward lower angles is observed, indicating the Au intake by the tubular micelles. This fact could suggest that it is preferable for the soft micellar structure to expand rather than protrude to accommodate the metallic particles, and so does the mesopore structure. From the lowest concentration at which this effect is first observed, we can conclude that the influence of a single nanoparticle inclusion within the soft micellar structure extends over a distance of several hundred nanometers.

The presence of 2-nm-diameter gold particles could not be detected by PXRD. Reflections due to gold nanocrystals were observed for materials containing 5- or 20-nm particles. The reflections observed at 2θ values of 44.5° and 52° are characteristic of cubic phase gold particles and thus confirm the presence of metallic gold in the samples. Furthermore, the broad reflections indicate that the size of the particles is in the nanometer range, showing that no aggregation occurred.

Nitrogen Porosimetry and FT-IR Results. The BET surface area values are in the expected range for these mesoporous structures (see Table 1). The shape of the N_2 adsorption−desorption isotherms (Figure 3) reveals that the specimens possess well-ordered struc-

(20) As a control, reference samples were prepared by mechanical mixture of gold particles and the respective mesoporous silicate. A calculated amount of gold solution (containing nanoparticles of 2, 5, and 20 nm) was mixed with the silicate. After being stirred for 30 min, the mechanical mixture was dried and powdered. TEM pictures showed agglomerated particles definitely on the outer surface, providing further indirect evidence that the synthetic insertion of the nanoparticles leads to embedded particles.

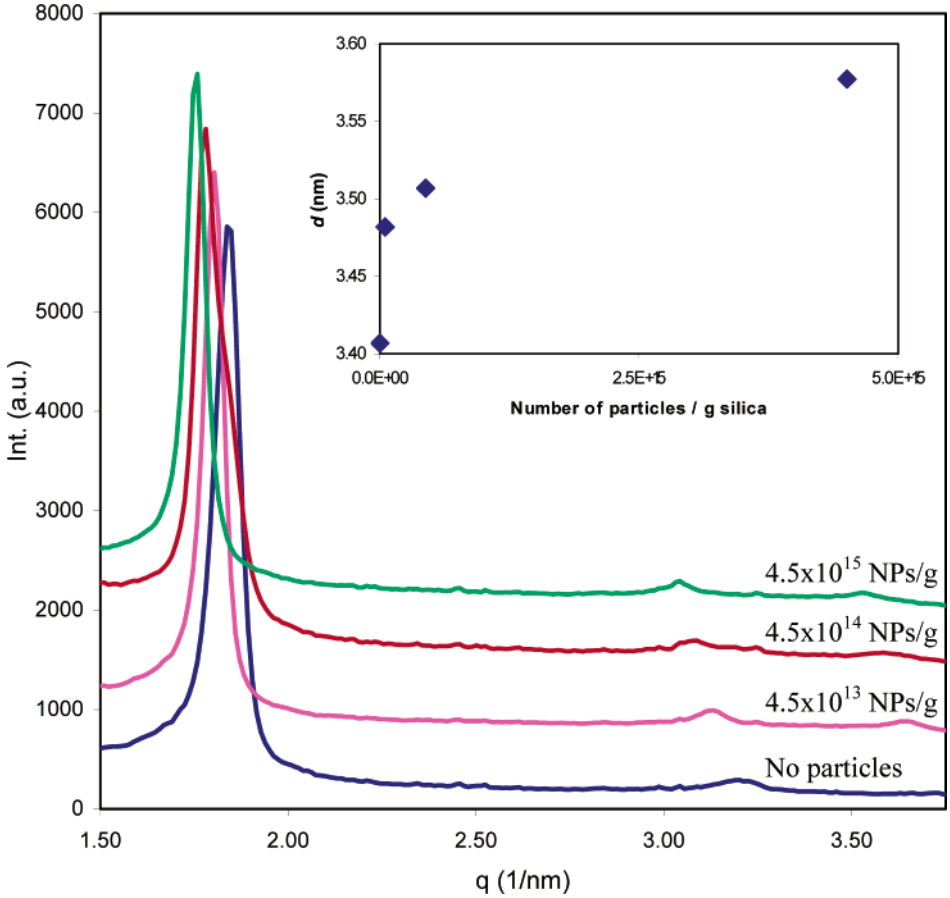

Figure 2. PXRD spectra of a series of MCM-41 samples with varying concentrations of 2-nm gold particles. Inset shows the mesoporous structure lattice spacing vs gold concentration curve.

tures. Little change in the pore structure of the materials upon gold particle incorporation was evident based upon nearly identical isotherms for the gold-containing samples compared to those of their respective parent mesoporous materials.[21] The adsorption and desorption BJH pore size distributions for the respective samples are shown in Figure 3 (inset). In support of the PXRD data, a narrow pore size distribution was evident for all of the samples, indicating that the highly ordered structures are maintained after incorporation of the gold nanoparticles.

As no systematic change either in the surface areas or in the shape of the adsorption−desorption isotherms was found, gold nanoparticles incorporated into the silicate material does not appear to alter the adsorption−desorption properties of small molecules such as nitrogen. This observation likely arises from (i) the relatively small number of nanoparticles that are contained within the materials and (ii) the fact that after template removal channels are larger than particles. A change in the adsorption−desorption properties of the materials would be expected in cases where the concentration of gold nanoparticles was high enough to efficiently block the pores.

Recording of the peak intensity of the intense methyl acetylene band at 2121 cm^{-1} attributed to molecules adsorbed onto a AuMCM-48 sieve indicates a small but significant drop of 12% in the case of the 5-nm sample compared to the 2-nm, 20-nm, and the Au-free sieve. This suggests reduced access of gas by blockage of the mesoporous channels by occluded Au particles. As expected, no such drop is observed in the case of the 2- and 20-nm samples. The observed 17% drop of methyl acetylene uptake of 5-nm AuMCM-41 when compared with the 2-nm, 20-nm, and Au-free samples is consistent with more efficient blockage in the case of the unidimensional channel system.

XANES Measurements. Alkanethiols are known to bond strongly to gold surfaces.[22] In principle, the presence of the Au nanoparticles inside the pores can be probed by monitoring a spectroscopic signal upon exposure of Au−containing MCM samples to thiol vapor in the presence or absence of the organic template. If the template is removed by calcination prior to exposure to thiol, the probe molecule is able to react with the Au surface if the metal nanoparticles are located in the molecular sieve pores. By contrast, no reaction with the metal particles is expected if the thiol is exposed to the uncalcined sieve; in this case, the very dense organic template may block access to the Au particles if these are located in the pores. Hence, a sulfur signal of a template-free AuMCM sieve would furnish positive evidence for the presence of metal particles in the mesopores.

Sulfur X-ray absorption spectroscopy is uniquely suited for monitoring thiol on metal particle surfaces

(21) Sing, K. S. W.; Everett, D. H.; Haul, R. A.; Moscou, L.; Pierottu, R. A.; Rouquerol, J.; Siemieniewska, T. *Pure Appl. Chem*. **1985**, *57*, 603. Gregg, S. J.; Sing, K. S. W. *Adsorption, Surface Area, and Porosity*, 2nd ed.; Academic: London, 1982.

(22) Finklea, H. O. *Electroanal. Chem*. **1996**, *19*, 109.

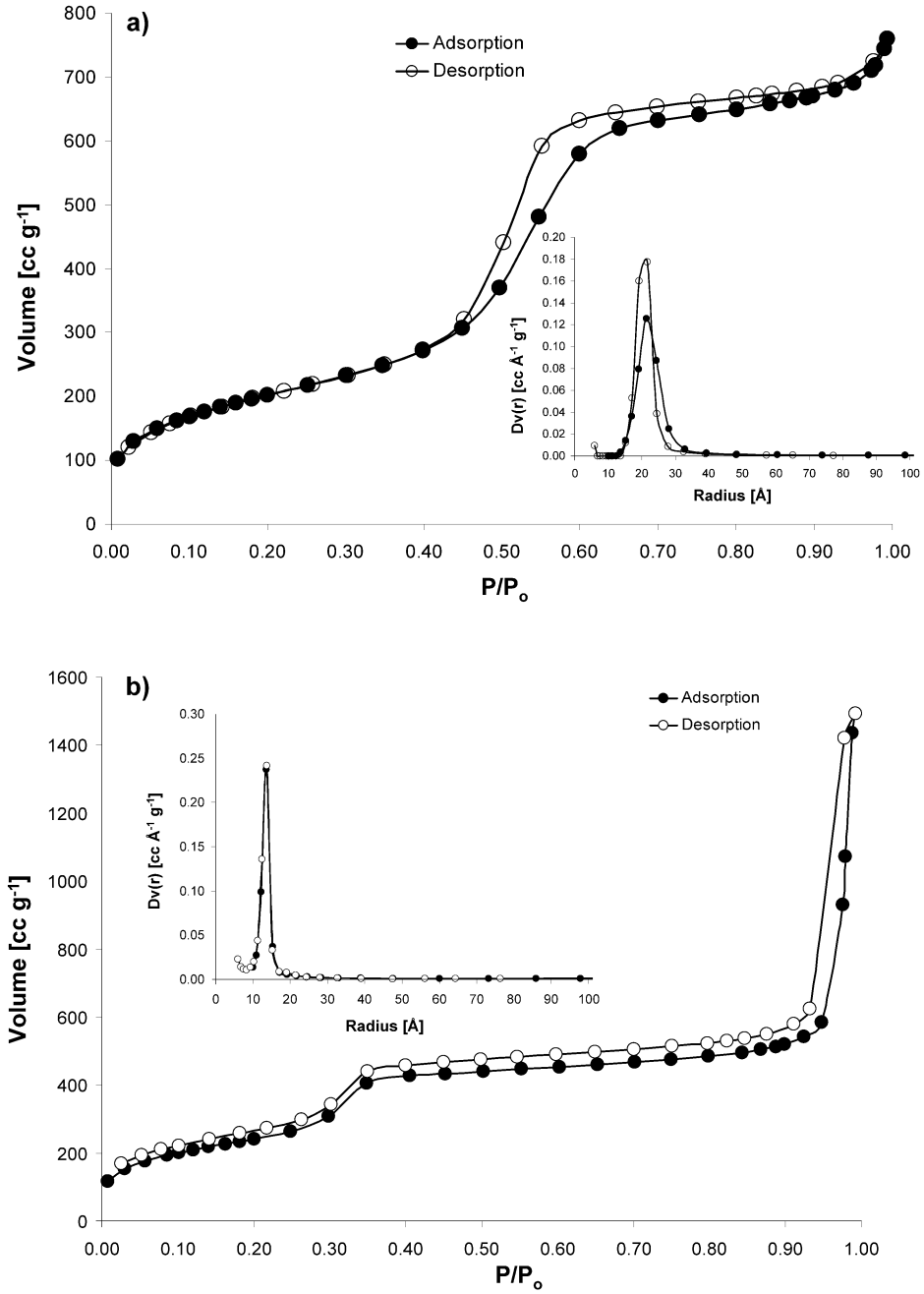

Figure 3. N_2 adsorption−desorption isotherms of (a) T-2 MCM-41 and (b) S-2 MCM-48 samples.

in the presence or absence of an organic template because the latter does not absorb spectroscopic light in the hard X-ray region. We exposed pressed wafers of MCM-48, AuMCM-48 (2 nm), AuMCM-48 (5 nm), and AuMCM-48 (20 nm) with and without organic template in the same glass vacuum container to 2 Torr of cyclohexyl mercaptane. Prior to loading, the samples were dehydrated by evacuation overnight (10^{-6} Torr). The exposed wafers were transferred to the X-ray absorption cell and evacuated at $<10^{-7}$ Torr.

Figure 4 shows the S-edge absorption of MCM-48 samples without Au (trace a), with 2-nm Au particles (trace b), and with 5-nm Au particles (trace c). Each spectrum is the difference of a calcined sample (without template) and the corresponding uncalcined sample (with template). Four scans were recorded and averaged for each sample. The sulfur absorption of the 2-nm AuMCM sample is approximately 3 times larger than the absorption of the sample with no gold. Since the template molecules are exclusively located inside the mesopores, the larger signal of the calcined 2-nm AuMCM-48 compared to the Au-free sample can only originate from thiol bound to the Au particles located in the pores. This constitutes conclusive evidence for the presence of 2-nm Au particles in the channels of MCM-48. The small residual absorption shown in Figure 4a for Au-free MCM-48 is attributed to thiol bound to defect sites of the silica surface. The sample with 2-nm Au particles contains a mere 140 pmol particles per wafer. Nevertheless, there is sufficient metal surface available for obtaining a detectable S signal. This does not hold for the 5- and 20-nm Au samples; for AuMCM-48 (5 nm),

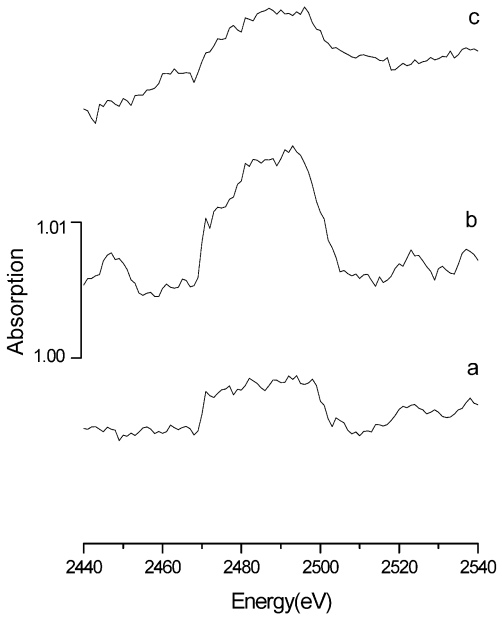

Figure 4. Sulfur K-edge XANES spectroscopy of (a) MCM-48, (b) AuMCM-48 (2 nm), and (c) AuMCM-48 (5 nm) samples exposed to 2 Torr cyclohexylmercaptane. Each trace represents the difference of the calcined sieve and the corresponding uncalcined sample.

the particle concentration is 30 times lower than that for the 2-nm sample. Although the Au surface area is 6 times larger for the 5-nm particles, there would be about 5 times fewer thiol molecules bound to the particles, making the S-edge signal difficult to detect, even if the particles were located in the pores. This is consistent with the observation that the signal of trace c is barely above that of the residual absorption of the Au-free sample (trace a). No difference was observed between the signals for the sieve with 20-nm Au particles and the one with no gold. While this in line with the expectation that 20-nm particles can only be located outside the MCM crystallites, no conclusions can be drawn from the measurements because the particle concentration is too low.

It is interesting to note that loading of a smaller and much more volatile sulfur compound, *tert*-butylthiol (40 Torr), led to intense S-edge bands for template-loaded AuMCM-48 (independent of particle size) as well as Au-free MCM-48 samples. A doublet with peaks at 2475 and 2480 eV is observed, which is absent in the template-free samples. Figure 5 shows these bands for uncalcined MCM-48. Hence, the new spectral features originate from butylthiol dissolved in the organic template. The fact that no such thiol was detected in the organic phase in the case of cyclohexylmercaptane confirms that this much less volatile molecule does not penetrate the organic assembly. It constitutes direct evidence that the densely packed template molecules block access of cyclohexylthiol to the pores of uncalcined samples. This strongly supports the assignment of the S absorption of the calcined Au (2-nm) sieve (Figure 4b) to cyclohexylmercaptane adsorbed on gold particles located in the pores.

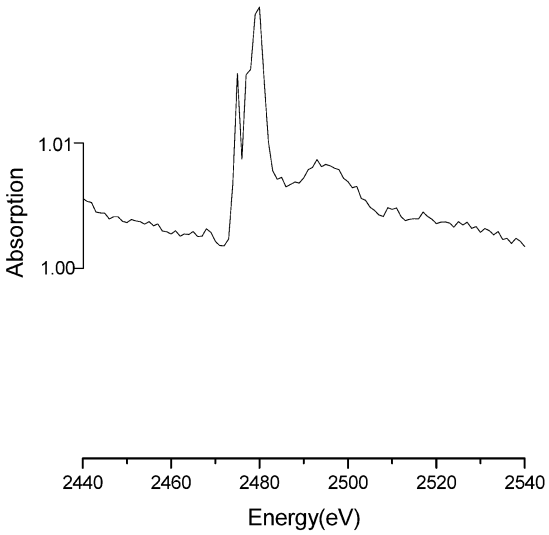

Figure 5. Sulfur K-edge XANES spectrum of uncalcined MCM-48 sieve exposed to 40 Torr *tert*-butylmercaptane. The trace represents the difference of the spectra of the uncalcined and calcined sample.

Conclusions

The successful encapsulation of uniformly sized gold nanoparticles in the mesoporous silicates MCM-41 and MCM-48 was reported. The encapsulated systems were made by growing the porous structure in the presence of the metal particles in an aqueous solution. The metal nanoparticle−mesoporous silicate system was characterized by a combination of physical techniques including powder X-ray diffraction, transmission electron microscopy, N_2 porosimetry, IR spectroscopy, and X-ray absorption near-edge spectroscopy. According to the PXRD spectra, the nanoparticles are inside the pores and act to expand the mesopore spacing; the lattice expansion depends on the nanoparticle size and also on the nanoparticle concentration. The shape of the N_2 adsorption−desorption isotherm revealed that the sample possesses well-ordered mesoporous structure and a narrow pore size distribution. X-ray absorption near-edge spectroscopy (XANES) was used in combination with the adsorption of thiols to provide conclusive evidence that the 2- and 5-nm-diameter Au nanoparticles are incorporated into the pores of the silicates and that they are accessible to reactant molecules.

Further studies on using other transition metal particles and other mesoporous structures are in progress.

Acknowledgment. This work was supported by the Director, Office of Energy Research, Office of Science, Divisions of Materials and Chemical Sciences of the U.S. Department of Energy under Contract no. DE-AC03-76SF00098 and NIH National Center for Research Resources, Grant no. 1 R01 RR-14891-01. We thank J. Pople, C. Liao, Q. Xu, and I. Sharp for assistance with the SAXS measurements at SSRL.

CM020824A